The endolysosomal adaptor PLEKHM1 is a direct target for both mTOR and MAPK pathways

Gubas, Andrea; Karantanou, Christina; Popovic, Doris; Tascher, Georg; Hoffmann, Marina E.; Platzek, Anna

Published in:
FEBS Letters

DOI:
10.1002/1873-3468.14041

Publication date:
2021

Document Version
Publisher's PDF, also known as Version of record

FEBS Letters

FEBS PRESS science publishing by scientists

The endolysosomal adaptor PLEKHM1 is a direct target for both mTOR and MAPK pathways

Andrea Gubas[1], Christina Karantanou[2,3], Doris Popovic[1], Georg Tascher[1], Marina E. Hoffmann[1], Anna Platzek[1], Nina Dawe[4], Ivan Dikic[1,5,6], Daniela S. Krause[2,3] and David G. McEwan[4,7]

1 Faculty of Medicine, Institute of Biochemistry II, Goethe University Frankfurt, Frankfurt am Main, Germany
2 Georg-Speyer-Haus, Institute for Tumor Biology and Experimental Medicine, Frankfurt, Germany
3 Goethe University Frankfurt, Frankfurt, Germany
4 Division of Cell Signalling & Immunology, School of Life Sciences, University of Dundee, UK
5 Buchmann Institute for Molecular Life Sciences, Goethe University Frankfurt, Frankfurt am Main, Germany
6 Max Planck Institute of Biophysics, Frankfurt am Main, Germany
7 Cancer Research UK Beatson Institute, Garscube Estate, Glasgow, UK

Correspondence
I. Dikic, Institute of Biochemistry II, Faculty of Medicine, Goethe University Frankfurt, Theodor-Stern-Kai 7, 60590 Frankfurt am Main, Germany.
D. S. Krause, Georg-Speyer-Haus, Institute for Tumor Biology and Experimental Medicine, Frankfurt, Germany
E-mail: krause@gsh.uni-frankfurt.de
David. G McEwan, Division of Cell Signalling & Immunology, School of Life Sciences, University of Dundee, Dundee, UK
E-mail: d.mcewan@beatson.gla.ac.uk

Andrea Gubas and Christina Karantanou equal contributing authors.

(Received 12 May 2020, revised 23 December 2020, accepted 28 December 2020)

doi:10.1002/1873-3468.14041

Edited by Lukas Alfons Huber

The lysosome is a cellular signalling hub at the point of convergence of endocytic and autophagic pathways, where the contents are degraded and recycled. Pleckstrin homology domain-containing family member 1 (PLEKHM1) acts as an adaptor to facilitate the fusion of endocytic and autophagic vesicles with the lysosome. However, it is unclear how PLEKHM1 function at the lysosome is controlled. Herein, we show that PLEKHM1 coprecipitates with, and is directly phosphorylated by, mTOR. Using a phosphospecific antibody against Ser432/S435 of PLEKHM1, we show that the same motif is a direct target for ERK2-mediated phosphorylation in a growth factor-dependent manner. This dual regulation of PLEKHM1 at a highly conserved region points to a convergence of both growth factor- and amino acid-sensing pathways, placing PLEKHM1 at a critical juncture of cellular metabolism.

Cell growth is a tightly regulated process, which is characterized by the balance between the synthesis and degradation of biomolecules, such as proteins, lipids and nucleotides. Two kinases are significant regulators of this process and integrate amino acid (mTOR; mechanistic target of rapamycin) and growth factor (MAPK; mitogen-activated protein kinase) signals for growth and survival [1,2]. Stimulation of receptor

Abbreviations
Deptor, DEP-domain-containing mTOR-interacting protein; EBSS, Earle's balanced salt solution; EGFR, epidermal growth factor receptor; GFP, Green fluorescent Protein; GST, Glutathione-S-Transferase; HOPS, homotypic fusion and vacuole protein sorting; mLST8, mammalian lethal with Sec13 protein 8; mTOR, mammalian target of rapamycin; PLEKHM1, Pleckstrin homology domain-containing family member 1; PRAS40, proline-rich AKT substrate of 40 kDa; Raptor, regulatory-associated protein of mTOR; Rictor, rapamycin-insensitive companion of mTOR; RTKs, receptor tyrosine kinases; SCV, *Salmonella*-containing vacuole; ULK1, Unc-51 like autophagy activating kinase; WT, Wild type.

tyrosine kinases (RTKs) by their cognate growth factor (e.g. epidermal growth factor receptor (EGFR) by EGF) results in dimerization of the RTK, transautophosphorylation, activation, recruitment of small GTPases and signal transduction through a cascade of kinases [2,3]. For example, EGF stimulation of EGFR leads to the activation of Ras GTPase, recruitment and activation of RAF kinase, then MEK (MAP kinase kinase; MKK) and then ERK 1/2 (MAPK). Activated ERK then phosphorylates a number of intracellular targets and simulates cellular proliferation [2,3].

In addition to stimulating MAPK, growth factor-mediated activation of RTKs activates the mTOR pathway. mTOR is a serine/threonine kinase and a catalytic subunit of two mTOR complexes – mTOR complex 1 (mTORC1) and mTOR complex 2 (mTORC2). The two protein complexes possess different functional properties since they interact with different accessory proteins. Cell growth is primarily controlled by mTORC1, whereas mTORC2 is involved in the regulation of cell proliferation and survival and is activated by growth factor stimulation of RTKs [1]. Both complexes share mTOR, mLST8 (mammalian lethal with Sec13 protein 8) and Deptor (DEP-domain-containing mTOR-interacting protein) as subunits [4,5], with mTORC1 also containing Raptor (regulatory-associated protein of mTOR) and PRAS40 (proline-rich AKT substrate of 40 kDa), as additional subunits [6–9]. mTORC2 contains Rictor (rapamycin-insensitive companion of mTOR), mSIN1 and Protor [10–12].

mTOR signalling is essential for monitoring nutrient availability in cells, and it has a central function in the process of autophagy [1]. mTORC1 is localized to the lysosomal surface during nutrient-rich conditions, where it interacts with Rag GTPases through Raptor [13]. During periods of amino acid starvation, mTORC1 is inhibited, leading to its dissociation from Rags, and therefore the lysosome; in contrast, mTORC2 couples growth factor and cytokine signalling to mTORC1 functions through direct phosphorylation of AKT [14] and is responsive to amino acids through the PI3K/AKT pathway [15]. mTORC1 suppresses autophagy flux through phosphorylation of the ULK1 (Unc-51 like autophagy activating kinase) complex that is restored upon mTOR inhibition [16,17]. Inhibition of mTORC1 leads to ULK1 activation and subsequent activation of the autophagy pathway through recruitment and phosphorylation of several downstream proteins, resulting in the generation of a double-membraned vesicle, the autophagosome [18–22]. The autophagosome sequesters the cargo marked for degradation and subsequently fuses with the lysosome where the cargo is degraded to recycle protein and lipid components back into the cytosol, re-activating mTOR [23].

The lysosomes act as a recycling hub for proteins and organelles, as well as a point of convergence for endosomal and autophagy pathways. Previously, we and others have identified that PLEKHM1 (Pleckstrin homology domain-containing family member 1) is an adaptor protein linking both endocytic and autophagy pathways through its interaction with Rab7, HOPS (homotypic fusion and vacuole protein sorting) and Arl8b [24–27]. HOPS is a tethering complex involved in the fusion of endocytic vesicles and is comprised of six subunits – VPS39, VPS41, VPS11, VPS16, VPS18 and VPS33. Rab7 and Arl8b are GTPases, involved in the transport and fusion of late endocytic/autophagy vesicles. PLEKHM1 directly binds Rab7, facilitating its own recruitment to the membranes [25], while its binding to Arl8b promotes its lysosomal localization and facilitates its interaction with HOPS complex [27]. In order to fulfil its function as an adaptor in endosome/lysosome pathway, PLEKHM1 requires simultaneous binding to both Rab7 and Arl8b [27]. However, the regulation of PLEKHM1 function and the dynamics of its intricate association with lysosomes is yet to be understood. Various mass spectrometry screens have reported phosphorylation sites on PLEKHM1; however, none of them explore in depth the consequences of such post-translational modification (phosphosite.org). Using a quantitative mass spectrometry approach, we discovered that PLEKHM1 interacts with mTOR and is directly phosphorylated at two proline-directed serine motifs within a highly conserved region of PLEKHM1 located between the RUN and first PH domain. Furthermore, we demonstrate that these sites match a MAPK consensus sequence (PxSP) and are also direct targets for MAPK-mediated phosphorylation. Using a phosphospecific antibody, we show that the inhibition of mTOR and MAPK decreases phosphorylation of PLEKHM1 at Ser432/Ser435. Our data suggest direct implication of mTOR and MAPK in regulating PLEKHM1 phosphorylation, and potentially its function, at the late endosome/lysosome, hinting that PLEKHM1 sits at the regulatory crossroads of these two essential signalling pathways.

Materials and Methods

Materials

See also Table S1. cDNA, antibodies. Plasmids used in this study are described in Table S1. *PLEKHM1* point

mutations were introduced by PCR and site-direct mutagenesis. GST-PLEKHM1 aa418-453 was generated by conventional cloning into pGEX-4T1. DNA sequences were verified by Sanger sequencing. The following antibodies were used in this study: Rabbit antibodies – anti-PLEKHM1 (in-house IG1132 [26]; and Sigma-Aldrich, Gillingham, UK, HPA025018, for immunofluorescence); anti-GFP (Living colors, Clontech, Takara-Bio Europe, Saint-Germain-en-Laye, France, Cat #632460); anti-mTOR (clone 7C10, CST, 2983S); anti-Raptor (clone 24C12, CST, 2280S); anti-Rictor (clone 53A2, CST, 2114); anti-phospho p70S6K (T389) (CST, 9234S); anti-p70S6K (CST, 9202); anti-phosphoserine (Millipore, Watford, UK, AB1603); anti-phosphoPLEKHM1 S432/S435 (in-house) was generated by Immunoglobe® GmbH by immunization of rabbits using a single degenerate synthetic peptide of PLEKHM1 spanning the region 427–439 (Ac-KLVV(S/pS)(pS)P(T/pT)(pS)PKNKC-NH2). Two rabbits were given two additional immunizations and bled, and the final phospho-PLEKHM1 (Ser432/Ser435; IG-1364) was purified against columns of dephosphorylated peptide and also single phospho-entities (PS432 and pS435 separately), anti-phosphoERK1/2 (T-202/Y204) (CST, 4370); anti-ERK1/2 (CST, 4695); anti-mLST8 (GβL; CST, 3274); anti-VPS41 (Santa Cruz, sc-377118); antivinculin (Sigma-Aldrich, V4505); anti-LAMP2 (clone H4B4; DSHB); anti-GST (Sigma-Aldrich, G1160); anti-HA (Roche, 11867423001); and anti-LAMP2 (DSHB, ABL-93-c). Secondary HRP-conjugated antibodies, goat anti-rabbit and goat anti-mouse, were used for immunoblotting. Alexa-conjugated 647 (mouse) and Alexa-555 rabbit secondaries were used for immunofluorescence studies (Invitrogen).

Cell culture

HeLa Kyoto [52] and U2OS cells were obtained from ATCC and grown in full medium (DMEM supplemented with 10% foetal bovine serum, 1% non-essential amino acids, 1% sodium pyruvate and penicillin/streptomycin). HeLa FlpIn-TREx PLEKHM1-GFP cells were previously described [26]. Protein expression was induced by 1 $\mu g \cdot mL^{-1}$ doxycycline. U2OS cells with endogenous GFP-PLEKHM1 were generated using CRISPR/Cas9-mediated modification of human PLEKHM1 (NM_014798.3) using the Cas9 D10A 'nickase' mutant. Optimal sgRNA pairs were identified and chosen on the basis of being as close as possible to the point of GFP insertion while having a low combined off-targeting score (sgRNA 1 5′-GATGACACC TGAAGAGACAGA-3′ and sgRNA2 5′-TACTTGCTG CACCACTACTTAGG-3′). The antisense guide (sgRNA2) was cloned onto the spCas9 D10A expressing pX335 vector (Addgene plasmid no. 42335) and the sense guides (sgRNA1) into the puromycin-selectable pBABED P U6 plasmid (Dundee-modified version of pBABE-puro plasmid). A donor construct consisting of GFP flanked by approximately 500-bp homology arms was synthesized by GeneArt (Invitrogen, Life Technologies, Paisley UK); each donor was engineered to contain sufficient silent mutations to prevent recognition and cleavage by Cas9 nuclease. The U2OS cells were transfected with both sgRNA and donor constructs and selected in 1 $\mu g \cdot mL^{-1}$ puromycin for 48 h, retransfected and allowed to recover in puromycin-free full medium. When confluent, cells were single-cell sorted for GFP-positive populations and homozygous clones selected for further analysis. MEFs expressing HA-PLEKHM1 were generated through retro-viral transduction with MSCV-N-Flag-HA-IRES-PURO-PLEKHM1-WT and selected using 2 $\mu g \cdot mL^{-1}$ puromycin. Where indicated, cells were incubated in Earle's balanced salt solution (EBSS) medium to induce amino acid starvation; or treated with Bafilomycin A1 (200 nm) or chloroquine (20 μm) to block fusion with lysosomes; torin 1 (250 μm) or Ku-0063794 (10 μm) (both from Tocris) to inhibit mTOR activity; or U0126 (10 μm) (Promega, Southampton, UK) to inhibit MAP kinases, for the time indicated in the figure legends. Transient transfection of HeLa cells was performed using TurboFect, according to the manufacturer's instructions.

Immunoprecipitation

Cells were lysed in CHAPS lysis buffer (50 mm Tris/HCl [pH 7.5], 0.5% CHAPS, 115 mm NaCl and 5 mm $MgCl_2$) supplemented with EDTA-free protease inhibitor cocktail (Roche) and phosphatase inhibitor cocktail (Sigma). Lysates were cleared by centrifugation, and the clear supernatant was incubated with primary antibody, rotating overnight at 4°C, followed by incubation with protein A sepharose beads (1 h with rotation at 4 °C), for endogenous immunoprecipitation, or with either GFP-TRAP beads (ChromoTek GmbH, Martinsried, Germany) or HA-affinity matrix (Sigma) for 30 min, rotating at 4°C. Pellets were washed three times with lysis buffer and four times with wash buffer (50 mM Tris/HCl [pH 7.4], 150 mM NaCl, 2 mM $MgCl_2$ and 0.1% Triton X-100). Proteins were eluted in 2x Laemmli sample buffer and subjected to SDS/PAGE and western blotting.

Western blotting

CHAPS (50 mm Tris/HCl [pH 7.5], 0.5% CHAPS, 115 mm NaCl, and 5 mm $MgCl_2$) or total cell lysis buffer (50 mm Tris/HCl [pH 7.4], 5 mm $MgCl_2$, 150 mm NaCl, 1% SDS), supplemented with EDTA-free protease inhibitor cocktail (Roche) and phosphatase inhibitor cocktail (Sigma), was used for cell lysis. Phosphatase inhibitors were omitted from samples treated with lambda-phosphatase. Lysates were cleared by centrifugation. For dephosphorylation of PLEKHM1, either whole cell lysates or PLEKHM1 immunoprecipitated on GFP-TRAP beads were incubated with 1 μL of lambda-phosphatase (NEB) with the

accompanying manufacturer's 10x phosphatase buffer and 1 mM $MnCl_2$, for 30 min at 30 °C. 2x Laemmli sample buffer was added to samples to stop the reaction. Proteins were resolved in 7% polyacrylamide gels or 5% polyacrylamide containing 20 μM Phos-Tag (Nard) and 10 mM $MnCl_2$, for protein mobility shifts. The proteins were then transferred onto a 0.2-μm PVDF membrane (Merck Millipore). Following incubation with primary and secondary antibodies, the blots were developed by ImmunoCRUZ western blotting Luminol reagent (Santa Cruz). Quantification was performed with FIJI/IMAGEJ software.

Mass spectrometry

Sample preparation for mass spectrometry

For testing of interaction partners, PLEKHM1-GFP was immunoprecipitated in HeLa FlpIn-TREx PLEKHM1-GFP cells on GFP-TRAP beads. Additionally, for detection of phosphorylation sites, SILAC labelling was used. HeLa FlpIn-TREx PLEKHM1-GFP cells were cultured in DMEM supplemented with either L-arginine $^{12}C_6$ $^{14}N_4$ (Arg0) and L-lysine$^{12}C_6$ $^{14}N_2$ (Lys0) or L-arginine $^{13}C_6$ $^{15}N_4$ (Arg10) and L-lysine-U$^{13}C_6$ $^{15}N_2$ (Lys8) as previously described (Ong et al., 2002). SILAC-labelled cells were lysed in CHAPS lysis buffer. PLEKHM1-GFP expression was induced for 16h with doxycycline, and HeLa FlpIn-TREx cells, cultured in light SILAC-labelled medium, were treated in EBSS for 4 h to starve cells of amino acids. PLEKHM1-GFP was immunoprecipitated using GFP-TRAP, and eluates were mixed 1:1 (v/v) and run on an SDS/PAGE gel. After excision of individual gel bands and destaining according to manufacturer´s instructions, proteins were reduced with 10mM DTT for 45 min at 56 °C and alkylated with 55mM Iodoacetamide for 30 min at RT under light protection. After digestion with Trypsin at 37 °C overnight, tryptic peptides were extracted from the gel pieces consecutively with 30% acetonitrile (ACN) containing 3% trifluoroacetic acid (TFA), then 80% ACN containing 0.1% TFA and finally 100% ACN for 30 min each. Extraction solutions were combined and dried by vacuum centrifugation before reconstitution in 0.1% formic acid for LC-MS/MS analysis.

LC-MS analyses

Peptides were analysed on an Orbitrap Elite mass spectrometer coupled to an easy nLC II (Thermo Fisher Scientific, Paisley, UK) using a 20 cm long, 75 μm ID fused-silica column, which has been packed in house with 3 μm C18 particles (ReproSil-Pur, Dr. Maisch), and kept at 45°C using an integrated column oven (Sonation). Peptides were eluted by a non-linear gradient from 8–40% acetonitrile over 240 min and directly sprayed into the mass spectrometer via a nanoFlex ion source (Thermo Fisher Scientific) at a spray voltage of 2.3 kV. Full scan MS spectra (300–2000 m/z) were acquired at a resolution of 120,000 at m/z 200, a maximum injection time of 100 ms and an AGC target value of 1×10^6 charges. Up to 20 most intense peptides per full scan were isolated in the ion-trap using a 2 Th window and fragmented using collision-induced dissociation (CID, normalized collision energy of 35). MS/MS spectra were acquired in rapid mode using a maximum injection time of 25 ms and an AGC target value of 5 x 10^3. Ions with charge states of 1 and > 6 as well as ions with unassigned charge states were not considered for fragmentation. Dynamic exclusion settings were 1 repeat count and 30-s repeat duration as well as an exclusion duration of 90s in order to minimize repeated sequencing of already acquired precursors.

Mass spectrometry data processing

Mass spectrometry raw data processing was performed with MaxQuant (v 1.3.0.5) applying default parameters. Acquired spectra were searched against the human reference proteome (Taxonomy ID 9606) downloaded from UniProt (09-2012) and a collection of common contaminants (244 entries) using the Andromeda search engine integrated in MaxQuant [53,54]. Identifications were filtered to obtain false discovery rates (FDR) below 1% for both peptide spectrum matches (PSM; minimum length of 7 amino acids) and proteins using a target-decoy strategy [55]. See Data S1 for analysis. Raw data are available via ProteomeXchange with identifier PXD021199.

Confocal microscopy

U2OS cells endogenously expressing GFP-PLEKHM1 were seeded on glass coverslips and, on the following day, starved in EBSS or treated with Bafilomycin A1 for the time periods indicated in the figure legends. Cells were then fixed in 4% paraformaldehyde (PFA; Santa Cruz, 30525-89-4) for 12 min minimum. Cells were permeabilized with 0.1% saponin in PBS at room temperature, followed by incubation with the primary antibodies in 0.1% saponin/5% BSA (bovine serum albumin)/PBS (phosphate-buffered saline). The coverslips were washed three times in 0.1% saponin/PBS, before being incubated with the secondary antibodies and DAPI (Molecular Probes, Lifetechnologies, Paisley, UK) for 1 h in 0.1% saponin/5% BSA/PBS. For detection of endogenous GFP-PLEKHM1, nanobody boosters towards GFP (anti-GFP, Atto-488 coupled, Chromotek; gba488-100) were used to enhance the signal. After incubation in secondary antibodies, the coverslips were washed twice in PBS/0.1% saponin, once in PBS and once in ddH_2O to remove residual saponin prior to mounting in ProLong Diamond Antifade containing Mowiol (Invitrogen, p36965). Cells were imaged using a Zeiss 710 confocal microscope with a 63 × objective lens. Subsequent image analysis was performed using FIJI/IMAGEJ [56].

Protein expression and purification

GST-PLEKHM1 aa418-453 was cloned into pGEX-4T-1 (GE Healthcare) and expressed in *E. coli* BL21 (DE3) cells in LB medium. Expression was induced by addition of 0.5 mM IPTG, and, subsequently, cells were incubated at 16°C overnight. Harvested cells were lysed using sonication in a lysis buffer (20 mM Tris/HCl [pH 7.5], 10 mM EDTA, 5 mM EGTA, 150mM NaCl), and the supernatant was subsequently applied to Glutathione Sepharose 4B beads (GE Healthcare, Hatfield, UK). After several washes, fusion protein-bound beads were used directly in the kinase assay.

In vitro kinase assay

Purified GST-tagged PLEKHM1 (aa 418-453) was washed 3 times in kinase buffer (10 mM HEPES, [pH 7.5], 50 mM NaCl, 50 mM β-glycerophosphate, 1 mM dithiothreitol [DTT], 10 mM $MgCl_2$, 4 mM $MnCl_2$) and subsequently incubated with 300 ng of a catalytic fragment (spanning amino acids 1362 to 2549) of human mTOR kinase (40061; BPS Bioscience) in the presence or absence of ATP (100 μM) for 1 h at 30 °C. 250 nM torin 1 was used to inhibit the *in vitro* kinase activity. For MAPK *in vitro* assay, ERK2 WT or kinase dead (D168A) (10 ng/100 μL reaction) was activated by incubating with MEK (10 ng/100 μL reaction) in kinase buffer (100 mM NaCl, 50 mM Tris/HCl, pH 7.0, 10 mM MgCl2, 100 mM ATP and 0.1% bovine serum albumin) for 30 min at 30° C. Recombinant GST-PLEKHM1 was added with additional cold ATP (100 μM), and the reaction was continued for 30 min at room temperature. After incubation, the reaction was stopped by adding 2x Laemmli buffer and by boiling at 95 °C for 5 min prior to SDS/PAGE and western blot analysis.

Statistical analysis

Results were plotted and analysed using GraphPad Prism software using the statistical method outlined in the figure legends.

Results

PLEKHM1 is found in complex with mTOR

Previously, we identified PLEKHM1 as an interaction partner of Rab7 [25] and subsequently showed that PLEKHM1 is present on LAMP1/LAMP2/Rab7-positive vesicles, which facilitates the fusion of autophagosomes and lysosomes [26] and influences the *Salmonella*-containing vacuole (SCV) formation [25]. As PLEKHM1 localizes at the lysosomal compartment through its interaction with Rab7 [27], we performed mass spectrometry analysis of the PLEKHM1 interactome using a Zwitter-ionic buffer (CHAPS) that enriches membrane-bound proteins, to gain a better understanding of the role of PLEKHM1 in this compartment. We performed SILAC-based LC-MS-MS on trypsinized immunoprecipitated complexes derived from HeLa-TREX cells expressing WT PLEKHM1-GFP (HEAVY) under doxycycline control for inducible expression and compared the interactome to un-induced cells (LIGHT). Using this method, we detected a number of late endocytic and lysosome-associated proteins (Fig. 1A), including Rab7, LAMP1 and LAMP2, in addition to HOPS complex and multiple SNAREs (Fig. 1A) [25,26]. These were found readily in our interactome and served as validation of the assay (Fig. 1A). Given our interest in the regulation of PLEKHM1 and the quantitative nature of LC-MS-MS, we observed a distinct subset of interaction partners of which mammalian target of rapamycin (mTOR) was one of the most abundant. Using the number of unique peptides detected (arrow thickness Fig. 1A), we pinpointed a strong interaction between mTOR and PLEKHM1 (Fig. 1A). As mTOR is known to localize to lysosomes and regulate autophagy [1], we focused our studies on components of the mTOR signalling pathway. We were able to identify components of the mTORC1 complex (Raptor),

Fig. 1. (A) Schematic representation of a subset of PLEKHM1 interacting partners as detected by mass spectrometry following immunoprecipitation of PLEKHM1-GFP using GFP-trap. The arrow thickness is proportional to the number of unique peptides detected by mass spectrometry. (B) HeLa FlpIn TREx cells stably expressing PLEKHM1-GFP were stimulated with 1 $\mu g \cdot mL^{-1}$ doxycycline 24 h before lysis. The cells were lysed in CHAPS buffer and subjected to GFP-trap co-immunoprecipitation, followed by SDS/PAGE and western blotting and probed with the indicated antibodies. Blots are representative of $n = 3$ independent experiments. (C) Representative confocal micrographs of CRISPR/Cas9-modified U2OS cells that express N-terminally GFP-tagged endogenous PLEKHM1 (GFP-PLEKHM1). Cells were either treated with full medium plus DMSO (FM) or Bafilomycin A1 (200nM) for 4 h to enlarge LAMP2-positive lysosomes. Cells were then fixed and counterstained with DAPI (blue; DNA), LAMP2 (magenta) and mTOR (red) and GFP-PLEKHM1 (green). Scale bar 10 μm. (D) Representative confocal micrographs of PLEKHM1-GFP HeLa FlpIn TREx cells that were left untreated (Full medium, FM, upper panels) or placed in complete starvation medium (starved) for 4 h before staining with LAMP2 (magenta) and mTOR (red) and visualization by confocal microscope. White box shows area of interest. Scale bar 10 μm. (E) Quantification of either mTOR/PLEKHM1 colocalization (red circles) or LAMP2/PLEKHM1 colocalization (blue squares) under either full media (FM) or starvation (starve) conditions. Mean ± SD of $n = 3$ independent experiments. ****$P < 0.0001$ Paired Student's *t*-test.

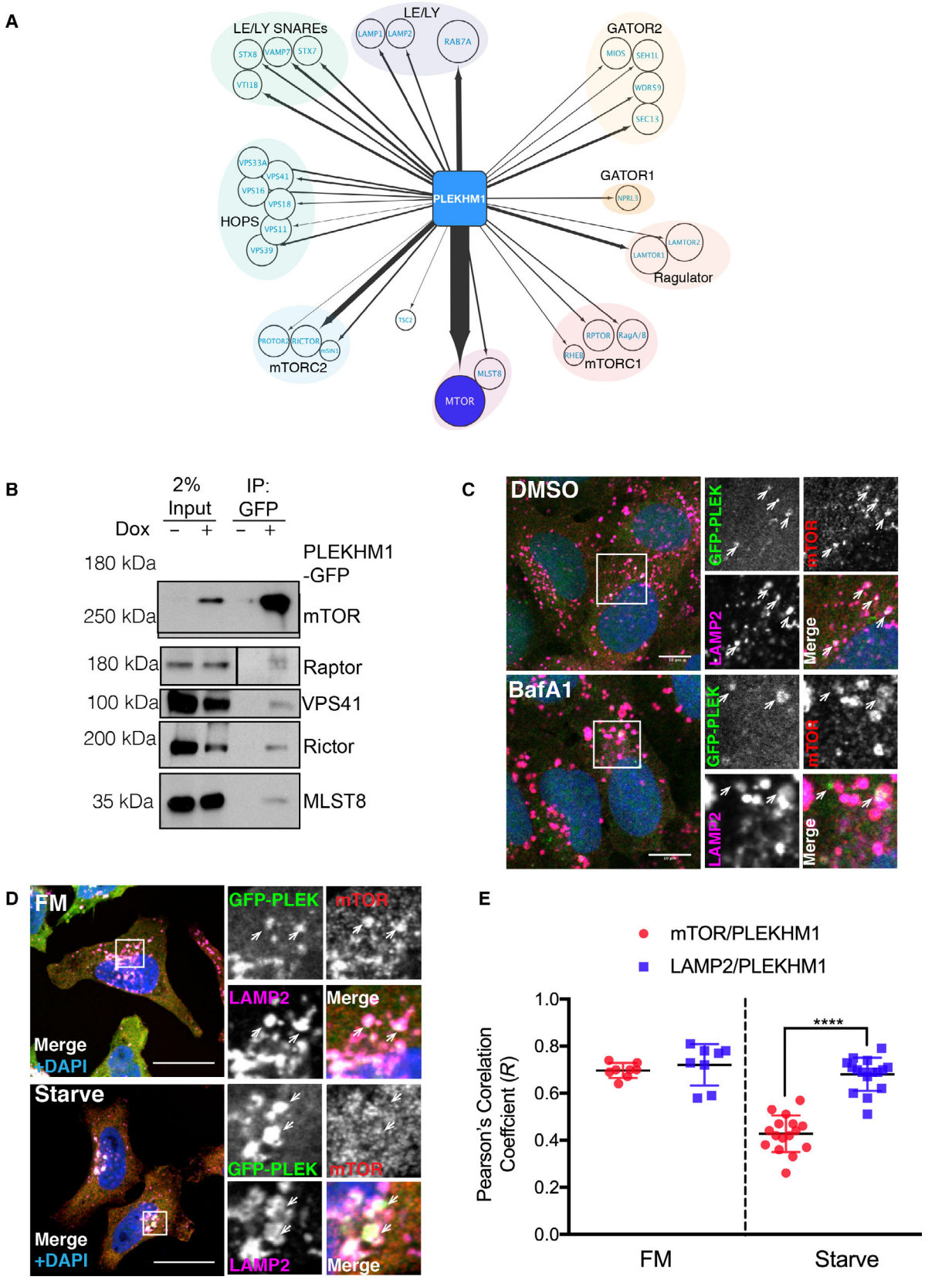

mTORC1 regulatory GTPases (Rheb, RagA/B), mTORC2 complex (Rictor, Protor), Ragulator (Lamtor1, Lamtor2), Gator1 (NPLR3) and Gator2 complex (MIOS, SEH1L, WDR59, SEC13), as well as the constitutive mTOR interaction partner mLST8 (Fig. 1A). PLEKHM1-GFP could coprecipitate with mTOR, Raptor, Rictor, mLST8 and VPS41 in doxycycline-induced HeLa-TREX cells, but not in un-induced immunoprecipitates (Fig. 1B). Using CRISPR/Cas9, we generated endogenous GFP-tagged PLEKHM1 (Fig. S1A) and could observe PLEKHM1 colocalizing with mTOR- on LAMP2-positive lysosomes (Fig. 1C, upper panels) that were enlarged upon Bafilomycin A1 treatment (V-ATPase inhibitor; Fig. 1C lower panels). Under nutrient-rich (full medium) conditions, we observed PLEKHM1-GFP (green) localized on LAMP2- (magenta) and mTOR- (red) positive vesicles (Fig. 1D upper panels and quantified in Fig. 1E). Upon amino acid starvation, PLEKHM1 was retained on LAMP2-positive vesicles, but mTOR became dispersed and reduced colocalization with PLEKHM1-GFP (Fig. 1D, lower panels, insets and quantified in Fig. 1E). Thus, PLEKHM1-GFP localizes and interacts with mTOR on the lysosome. Given the previously reported role of PLEKHM1 in facilitating the fusion of late endosomes and autophagosomes with the lysosome [25,26], we hypothesized that mTOR phosphorylates and potentially regulates PLEKHM1 at the lysosome to control its function.

mTOR directly phosphorylates PLEKHM1 at a conserved serine motif

mTOR is a key regulator of cellular metabolism, plays a key role in amino acid sensing at the lysosome and acts as one of the main 'on/off' switches for the autophagy pathway [16,17]. Therefore, we next asked whether PLEKHM1 is phosphorylated in an mTOR-dependent manner. To inhibit mTOR, we used either torin 1, or Ku-0063794, both of which are highly specific towards mTOR, and do not affect PI3K activity at the concentrations used [28,29]. Upon either mTOR inhibition with Ku-0063794 (KU) or starvation (EBSS) conditions, we could observe increased mobility shift of endogenous PLEKHM1, compared to full medium controls (Fig. 2A). After a period (4 h) of starvation and refeeding for 40 min in full medium, this increased mobility shift was reversed (Fig. 2A), implying that under these conditions PLEKHM1 may be post-translationally modified. Immunoprecipitation of endogenous PLEKHM1 and subsequent treatment with lambda-phosphatase (λ-PPase) resulted in increased mobility of the immunoprecipitated PLEKHM1 (Fig. 2B). Next, HeLa FlpIn-TREx cells were induced for 16 h overnight with doxycycline to express PLEKHM1-GFP and were treated for increasing time in starvation medium. The cells were subsequently lysed and run on a phos-tag gel. The inclusion of the phos-tag chelating agent in conventional polyacrylamide gels retards the migration of

Fig. 2. (A) Mouse embryonic fibroblasts (MEFs) were placed into either full medium (FM), full medium containing 10 μm Ku-0063794 (KU) for 4 h or EBSS medium (starved) for 4 h or EBSS for 4 hours followed by FM for 40 min. Cells were lysed and analysed by western blotting. Samples were blotted for endogenous Plekhm1, and anti-vinculin was used as a loading control. (B) Endogenous PLEKHM1 was immunoprecipitated from MEFs and either left untreated or treated with lambda-phosphatase (λ-PPase) for 30 min. Blots were probed with anti-PLEKHM1. (C) HeLa FlpIn TREx cells stably expressing PLEKHM1-GFP were stimulated by 1 mg·mL^{-1} doxycycline for 16 hours and either left untreated or treated for the times indicated with starvation media (EBSS). In addition, untreated lysate was treated with lambda-phosphatase (λ-PPase) for 30 mins. Total cell lysates were then run on either a 5% gel containing phos-tag (20 μM) or a 7% polyacrylamide gel and probed for the presence of PLEKHM1 and vinculin as a loading control. (D) HeLa FlpIn TREx cell stably expressing PLEKHM1-GFP was stimulated by 1 μg·mL^{-1} doxycycline for 16 h. The cells were then either left untreated, treated with phosphatase or starved for 20, 50 or 120 min, before being lysed in CHAPS lysis buffer and subjected to GFP-Trap Co-IP and western blotting. Blots are representative of $n = 3$ independent experiments. (E) Phosphorylated PLEKHM1 was calculated as a percentage of total PLEKHM1-GFP on the beads. *$P < 0.026$; ns = not significant, Student's *t*-test of $n = 3$ independent experiments. (F) HeLa FlpIn TREx cells stably expressing PLEKHM1-GFP were either left un-induced or stimulated by 1 μg·mL^{-1} doxycycline for 16 h and then treated with either DMSO, 10 μM Ku-0063794 (KU) or 10 μM Ku-0063794 (KU) plus 20 μM chloroquine (CQ) for 4 h. Cells were then lysed in CHAPS buffer, and anti-GFP-Trap beads were used to immunoprecipitate GFP-tagged PLEKHM1. An untreated IP was treated with lambda-phosphatase for 30 mins as control. Samples were then subjected to SDS/PAGE and analysed by western blotting using the indicated antibodies. Numbers shown indicate the percentage of phosphorylated PLEKHM1 or immunoprecipitated sample (mTOR, VPS41) compared with input or total IP. (G) The workflow for identification of PLEKHM1 phosphorylation sites by using SILAC-based mass spectrometry. (H) Schematic diagram showing the phosphosites identified that overlapped between starvation and Ku-0063794 treatments. Alignment of multiple species of PLEKHM1 in the region of Ser432/Ser435 (human PLEKHM1) shows the high degree of sequence conservation. (I) The mass spectrometric fragment ion scan of the peptide corresponding to phosphorylated Ser432 and Ser435 in LVVSSPTSPK

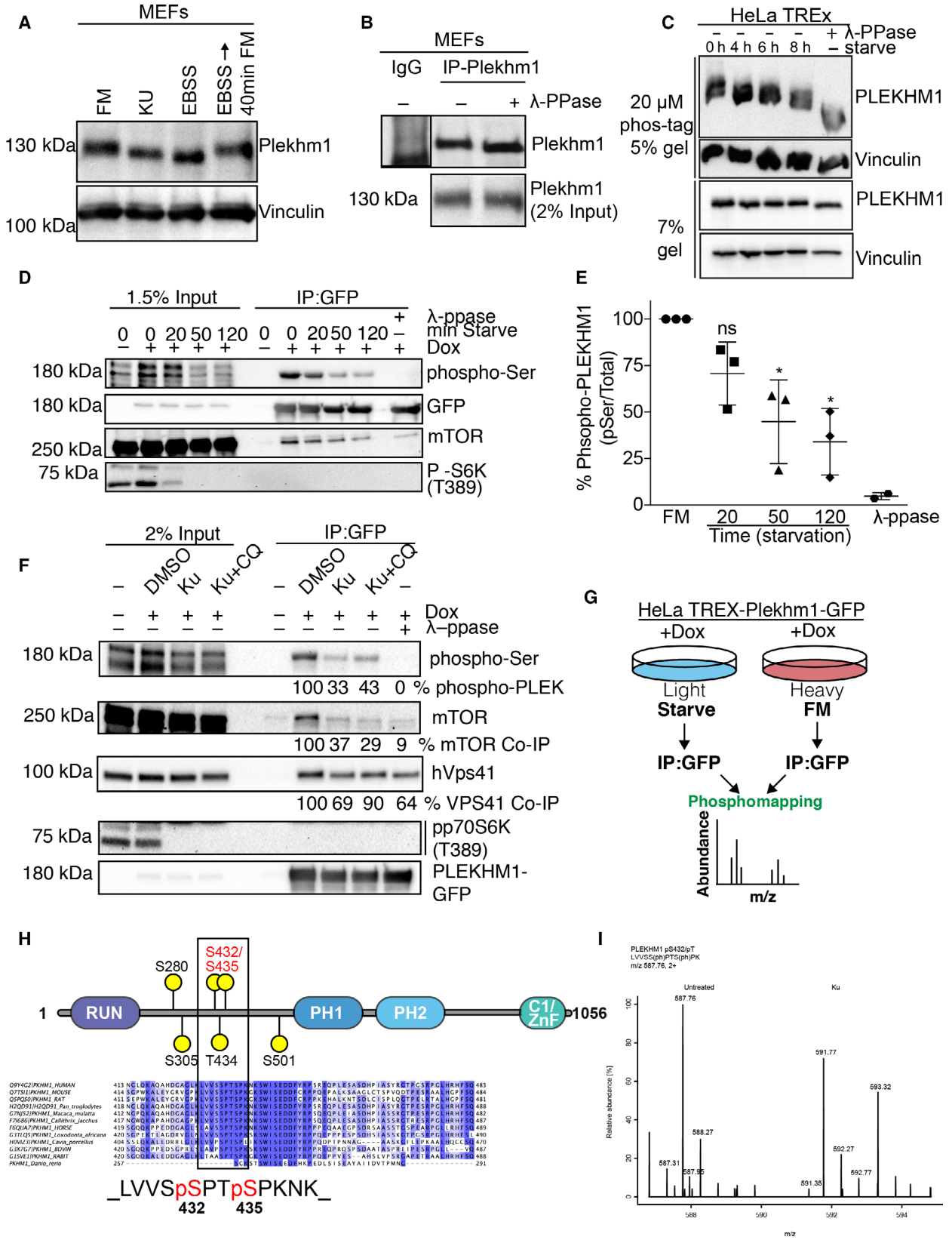
A
MEFs
FM
KU
EBSS
EBSS → 40min FM
130 kDa
Plekhm1
100 kDa
Vinculin
B
MEFs
IgG
IP-Plekhm1
– – + λ-PPase
Plekhm1
130 kDa
Plekhm1 (2% Input)
C
HeLa TREx
– – – – + λ-PPase
0 h 4 h 6 h 8 h – starve
20 μM phos-tag 5% gel
PLEKHM1
Vinculin
7% gel
PLEKHM1
Vinculin
D
1.5% Input
IP:GFP
λ-ppase
0 0 20 50 120 0 0 20 50 120 + min Starve
– + + + + – + + + + – Dox
180 kDa
phospho-Ser
180 kDa
GFP
250 kDa
mTOR
75 kDa
P -S6K (T389)
E
% Phospho-PLEKHM1 (pSer/Total)
100
75
50
25
0
ns
*
*
FM
20
50
120
λ-ppase
Time (starvation)
F
2% Input
IP:GFP
– DMSO Ku Ku+CQ – DMSO Ku Ku+CQ
– + + + – + + + + Dox
– – – – – – – – + λ–ppase
180 kDa
phospho-Ser
100 33 43 0 % phospho-PLEK
250 kDa
mTOR
100 37 29 9 % mTOR Co-IP
100 kDa
hVps41
100 69 90 64 % VPS41 Co-IP
75 kDa
pp70S6K (T389)
180 kDa
PLEKHM1-GFP
G
HeLa TREX-Plekhm1-GFP
+Dox
+Dox
Light
Starve
Heavy
FM
IP:GFP
IP:GFP
Phosphomapping
Abundance
m/z
H
S280
S432/ S435
1
RUN
PH1
PH2
C1/ ZnF
1056
S305
T434
S501
LVVSpSPTpSPKNK
432
435
I
PLEKHM1 pS432/pT
LVVS5(ph)PTS(ph)PK
m/z 587.76, 2+
Untreated
Ku
587.76
591.77
593.32
588.27
592.27
587.31
587.95
591.35
592.77
Relative abundance [%]
m/z

phosphorylated protein species and can help distinguish different states of phosphorylation of the protein of interest [30]. Phosphatase-treated PLEKHM1-GFP sample showed a large increase in mobility, and increasing time of mTOR inhibition showed a range of mobility shifts between the untreated (full medium) and phosphatase-treated (Fig. 2C). This indicates that PLEKHM1-GFP phosphorylation is decreased upon mTOR inhibition (Fig. 2C). Next, we induced PLEKHM1-GFP expression in HeLa-TREX cells and left the cells untreated or starved them of amino acids and growth factors for up to 2 h (starve). Using GFP-trap beads, we immunoprecipitated PLEKHM1-GFP and probed with a generic phosphoserine antibody and monitored the effect on PLEKHM1 phosphorylation. As a negative control, we treated immunoprecipitated PLEKHM1 for 30 min using λ-PPase to dephosphorylate PLEKHM1. Increased time in starvation medium resulted in decreased PLEKHM1 phosphorylation up to approximately 70% of total phosphorylated PLEKHM1 after 2 h of starvation (Fig. 2D and quantified in 2E). PLEKHM1 phosphorylation (using phosphoserine antibody) was decreased by almost 70% after treatment with 10 μM Ku-0063794 for 4 h (Fig. 2F). This was associated with decreased mTOR association with PLEKHM1 under these conditions (~60% loss of mTOR; Fig. 2F) that was not prevented by lysosome inhibition (chloroquine, CQ; Fig. 2F). The majority of VPS41 (HOPS complex) was still bound to PLEKHM1 under these conditions (~ 70% bound; Fig 2F). Next, we wanted to map potential PLEKHM1 phosphorylation sites that changed upon amino acid starvation and mTOR inhibition. Using SILAC (stable isotope labelling of amino acids in cell culture), to differentiate changes in phosphorylation status of PLEKHM1, we labelled doxycycline-induced PLEKHM1-WT cells with either LIGHT or HEAVY amino acids, and either starved (LIGHT) the cells or left them in full medium (HEAVY) for 2 h. We also compared the phosphorylation status of PLEKHM1-GFP in untreated (full medium + DMSO) versus KU-treated cells. We immunoprecipitated PLEKHM1-GFP using GFP-Trap beads and analysed by LC/MS to map-specific amino acid residues on PLEKHM1 that change upon amino acid depletion/KU treatment (Fig. 2G). In total, we mapped nine potential phosphorylation sites that decreased upon starvation or KU treatment. Of these sites, only Ser280, Ser305, Ser432, Thr434, Ser435 and Ser501 (Fig. S1B–G) overlapped between the two conditions (Starved and KU). Of particular interest were the clusters of phosphoserine/threonine around 431-435 on PLEKHM1 (Fig. 2H,I). These sites have also previously been found to be enriched in multiple independent mass spectrometry analyses (phosphosite.org). These include analysis of the ultradeep human phosphoproteome [31] and were found to be increased in a number of cancer cell types including breast cancer [32], non-small-cell lung cancer [33] and leukaemia [34]. Interestingly, Ser432/435 was shown to decrease upon rapamycin treatment [35], and the same sites have also been shown to be increased upon insulin treatment [36]. Therefore, due to the number of hits at these sites and due to the fact that this cluster of phosphoserine residues is present within a highly conserved region of PLEKHM1 (Fig. 2H; alignment), we wanted to verify that these were indeed mTOR-directed phosphorylation sites on PLEKHM1.

Fig. 3. HeLa cells transiently expressing PLEKHM1-GFP WT or PLEKHM1-GFP S432A/S435A were treated with EBSS for 4 h or left untreated and analysed by western blotting using the phosphospecific antibody against hPLEKHM1 S432/S435, GFP and phospho-p70S6K antibodies. Blots are representative of $n = 3$ independent experiments. (A) HeLa FlpIn TREx cells stably expressing PLEKHM1-GFP were either left un-induced or stimulated by 1 $\mu g \cdot mL^{-1}$ doxycycline for 16 h and then treated with either DMSO, 10 μM Ku-0063794 (KU), 250 nM torin 1 or starved for 4 h in EBSS medium. HeLa cells were transiently transfected with either PLEKHM1-GFP WT or PLEKHM1-GFP S432A/S435A as controls. Total cell lysates were then subjected to SDS/PAGE, and antibodies against phosphorylated PLEKHM1 (S432/S435), GFP (total PLEKHM1) and phospho-p70S6K (T389) were used. Blots are representative of $n = 3$ independent experiments. (B) MEFs stably expressing HA-PLEKHM1 (human) were either left in full medium (FM) or starved for 4 h in EBSS medium and lysed, and anti-HA was used to immunoprecipitate PLEKHM1. Samples were analysed using SDS/PAGE and western blotting for phospho-PLEKHM1(S432/S435) and anti-HA. Rabbit IgG was used as a control for immunoprecipitation. (C) Endogenous PLEKHM1 was immunoprecipitated from HeLa cells grown in either full medium (FM) or EBSS (4 h). Samples were then subjected to SDS/PAGE and western blotting and probed with phospho-PLEKHM1(S432/S435) and total PLEKHM1 antibodies. Levels of phospho-PLEKHM1 were calculated as a percentage and were normalized to total immunoprecipitated PLEKHM1 in each lane. Rabbit IgG was used as negative control for immunoprecipitation. Blots are representative of $n = 3$ independent experiments. (D) *In vitro* kinase assay using purified mTOR kinase and purified GST-PLEKHM1 418-453 fragment in the presence or absence of ATP. Blots are representative of $n = 3$ independent experiments. (E) U2OS cells overexpressing PLEKHM1-GFP WT (upper panels) or S432A/S435A (lower panels) were counterstained with anti-phospho-PLEKHM1 pS432/pS435 (red), anti-LAMP2 (magenta) and DAPI. Scale bar 10 μm.

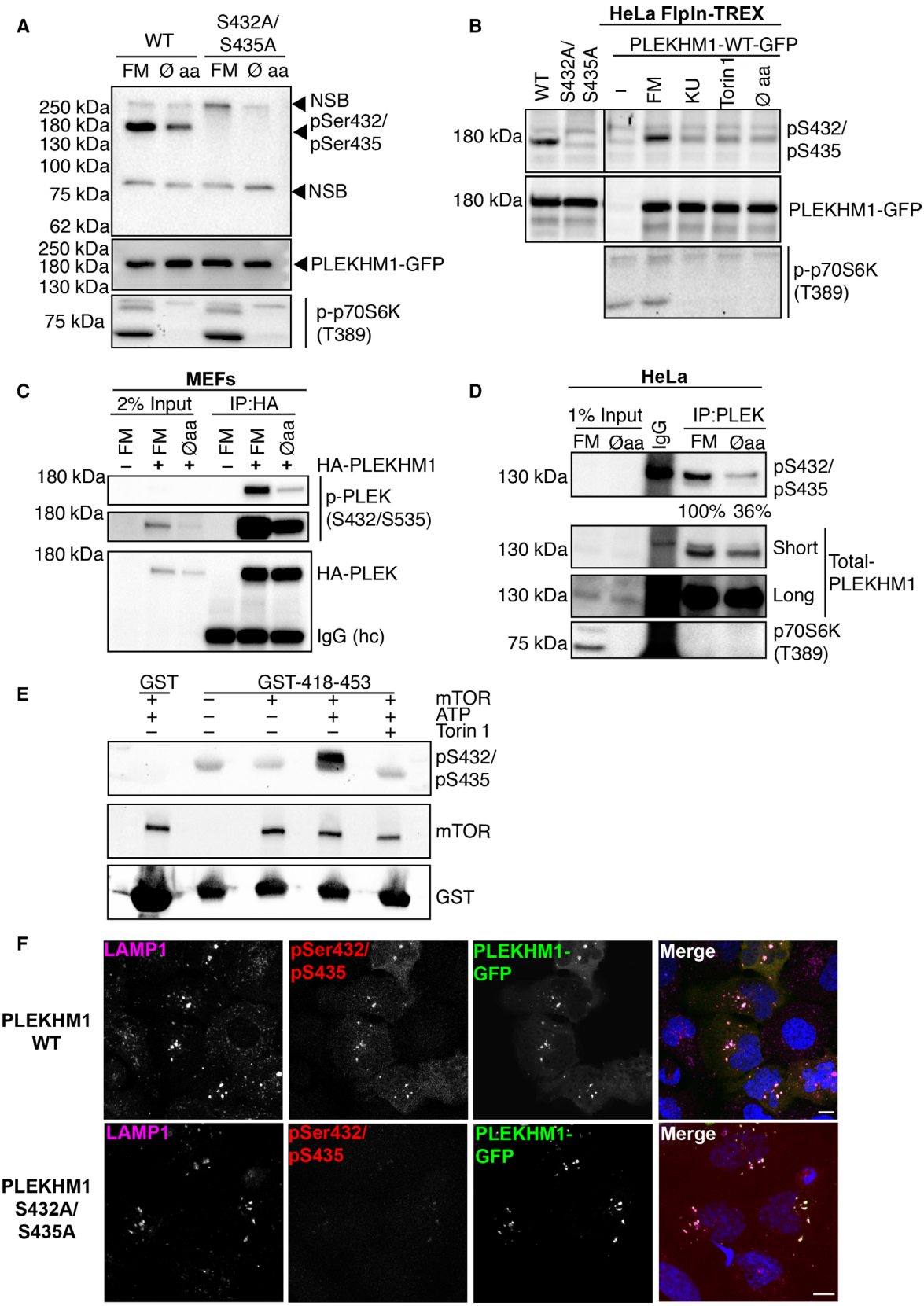
A
WT
S432A/
S435A
FM Ø aa FM Ø aa
250 kDa
180 kDa
130 kDa
100 kDa
75 kDa
62 kDa
NSB
pSer432/
pSer435
NSB
PLEKHM1-GFP
p-p70S6K
(T389)
B
HeLa FlpIn-TREX
PLEKHM1-WT-GFP
WT
S432A/
S435A
–
FM
KU
Torin 1
Ø aa
180 kDa
pS432/
pS435
PLEKHM1-GFP
p-p70S6K
(T389)
C
MEFs
2% Input
IP:HA
FM FM Øaa FM FM Øaa
– + + – + +
HA-PLEKHM1
p-PLEK
(S432/S535)
HA-PLEK
IgG (hc)
D
HeLa
1% Input
IgG
IP:PLEK
FM Øaa
FM Øaa
130 kDa
pS432/
pS435
100% 36%
Short
Long
Total-
PLEKHM1
p70S6K
(T389)
E
GST
GST-418-453
mTOR
ATP
Torin 1
pS432/
pS435
mTOR
GST
F
PLEKHM1
WT
PLEKHM1
S432A/
S435A
LAMP1
pSer432/
pS435
PLEKHM1-
GFP
Merge

PLEKHM1 is directly phosphorylated by mTOR

Next, we developed phosphospecific antibodies directed against a dual phosphorylated peptide of PLEKHM1 containing phosphorylated Ser432/Ser435. Upon transient transfection of the PLEKHM1 WT and Ser432A/Ser435A (2A) plasmids, we could show that the phosphospecific antibody only recognized phosphorylated PLEKHM1-WT and not the PLEKHM1 protein in which Ser432/Ser435 sites are mutated to alanine (Fig. 3A). Moreover, phosphorylation of PLEKHM1 at these sites decreased upon amino acid starvation in HeLa FlpIn-TREx cells overexpressing PLEKHM1-GFP (Fig. 3A), and phosphorylation at these sites was sensitive to torin 1, Ku-0063794 and amino acid starvation (Fig. 3B). We were also able to detect phosphorylated PLEKHM1 that was sensitive to amino acid starvation using mouse embryonic fibroblasts expressing HA-tagged PLEKHM1 (Fig. 3C). Importantly, we could detect endogenous levels of phosphorylated Ser432/435 PLEKHM1 in HeLa cells that was sensitive to amino acid starvation (Fig. 3D). Using bacterially purified GST-PLEKHM1 (amino acids 418-453) that contains the potential mTOR phosphorylation sites, we showed that purified mTOR can phosphorylate Ser432/435 *in vitro* as phosphorylation (as detected by pS432/pS435 antibody) was sensitive to the presence of ATP and torin 1 (Fig. 3E). Overexpression of WT PLEKHM1-GFP showed that PLEKHM1 is phosphorylated at S432/S435 on LAMP2-positive vesicles (lysosomes; (Fig. 3F, upper panels) and pS432/pS435 is lost when these sites are mutated (Fig. 3F, lower panels). Next, we wanted to test whether mutation of these phosphosites affected the previously identified interactions of PLEKHM1 [25,26,37]. We tested the interaction of overexpressed HA-tagged PLEKHM1 WT, 2A or 2D (S432D/S435D) with either GFP alone, GFP-Rab7 (Fig. S2 A-B) or GFP-GABARAP (Fig S2 C-D). Interestingly, neither mutant significantly affected the interaction of PLEKHM1 with either Rab7 or GABARAP. Moreover, overexpression of PLEKHM1-WT, 2A or 2D mutants did not have a dominant effect on LC3B lipidation or p62/SQSTM1 turnover, when overexpressed in HEK293T cells (Fig. S2E-G). Taken together, we show that the Ser432/435 sites are phosphorylated by mTOR are sensitive to conditions that alter mTOR activity and have an, as yet, undefined effect on PLEKHM1 function.

PLEKHM1 Ser432/Ser435 is MAPK target sites

The sites we identified as being phosphorylated by mTOR conform to the proline-directed mTOR consensus motif [38]. When we further inspected the phosphomotif within PLEKMH1, we realized that the same sites also conform to the PxSP MAPK-directed phosphorylation motif (Fig. 4A) [39,40]. This prompted us to explore whether these sites were also possible substrates of the MAPK pathway. Therefore, we tested whether PLEKHM1 phosphorylation could be induced in a growth factor/MAPK-dependent manner. MEFs expressing either vector only or HA-tagged PLEKHM1 were grown in 1% serum-containing medium for 16 h and subsequently stimulated with either full medium (FM) or with 50 ng/mL epidermal growth factor (EGF) for 0, 30, 60, 120 and 180 min. In the latter case, PLEKHM1 phosphorylation peak coincided with the peak in the activation of the MAPK

Fig. 4. (A) Schematic representation of identified PLEKHM1 phosphorylation sites that align to the proline-directed mTOR phosphorylation motif and PxSP MAPK phosphorylation motif. Inhibitors of both pathways are shown to distinguish the potential differences in phosphorylation. (B) MEFs overexpressing vector only or HA-PLEKHM1 were grown overnight in medium containing 1% serum and, subsequently, cultured in either full medium or FM containing 50 ng·mL^{-1} EGF. Cells were treated for the indicated times, and western blots were performed on total cell lysates using the indicated antibodies. (C) *In vitro* kinase assay using purified His-GST-tagged MEK (MKK1), GST-tagged-ERK2 (MAPK1) WT and -ERK2 kinase dead (D168A) using purified GST-PLEKHM1 418-453 fragment as substate in the presence or absence of ATP. Samples were probed with phospho-PLEKHM1(S432/S435), GST (ERK2), anti-His tag (MEK) and total PLEKHM1 input detected by ponceau S Blots are representative of n = 3 independent experiments. (D) MEFs overexpressing HA-tagged PLEKHM1 were grown overnight in medium containing 1% serum and subsequently cultured in medium containing 50 ng·mL^{-1} of the indicated growth factors (EGF, FGF, PDGF-AA/BB, IGF) with or without 10 μM U0126 or 250nM torin 1 for 30 min. For those cells treated with U0126 or torin 1, cells were preincubated for 1 h prior to growth factor treatment. Western blots were performed on total cell lysates using the indicated antibodies. (E) Representative western blots of MEFs expressing empty vector (V) or HA-tagged PLEKHM1 were grown in full medium (FM; DMEM) or FM plus 250 nM torin 1, 10 μM U0126 (UO) or 250 nM torin 1 plus 10 μM U0126 or EBSS. Total cell lysates were subjected to SDS/PAGE western blotting and probed with the indicated antibodies. (F) Quantification of (E). Percentages are calculated based on total versus phospho-PLEKHM1 (S432/S435). Horizontal bar represents mean ± SEM of $n = 3$ independent experiments (individual points on graph). One-way ANOVA statistical test. $^{**}P = 0.0050$; $^{***}P = 0.0006$; $^{****}P \leq 0.0001$; $^{*}P = 0.0336$ (torin 1 vs torin 1 + U0126); $^{*}P = 0.0253$ (U0126 vs torin 1 + U0126).

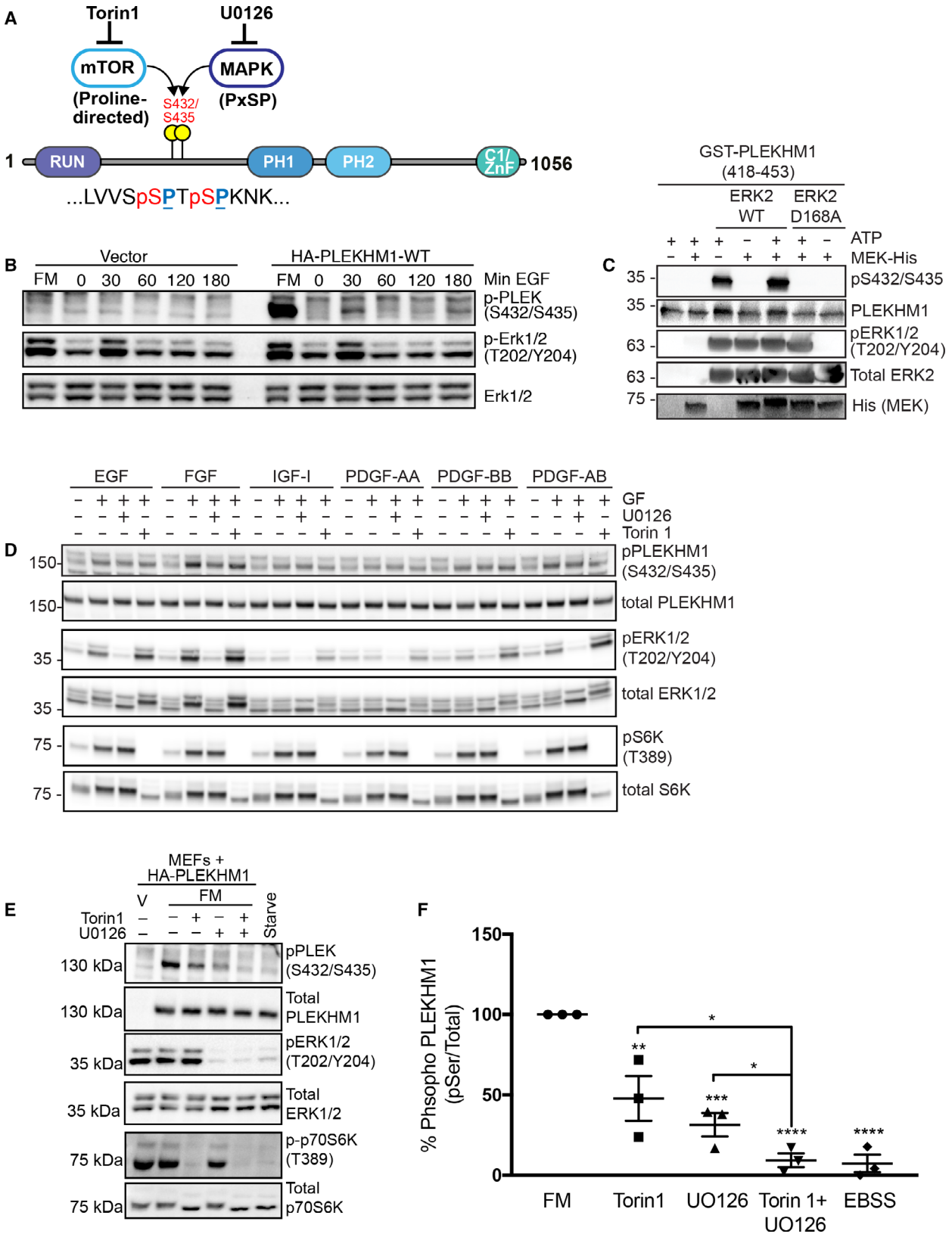
A
Torin1
U0126
mTOR
MAPK
(Proline-directed)
S432/S435
(PxSP)
1
RUN
PH1
PH2
C1/ZnF
1056
...LVVSpSPTpSPKNK...
B
Vector
HA-PLEKHM1-WT
FM 0 30 60 120 180
FM 0 30 60 120 180
Min EGF
p-PLEK (S432/S435)
p-Erk1/2 (T202/Y204)
Erk1/2
C
GST-PLEKHM1 (418-453)
ERK2 WT
ERK2 D168A
ATP
MEK-His
35
35
63
63
75
pS432/S435
PLEKHM1
pERK1/2 (T202/Y204)
Total ERK2
His (MEK)
D
EGF
FGF
IGF-I
PDGF-AA
PDGF-BB
PDGF-AB
GF
U0126
Torin 1
150
150
35
35
75
75
pPLEKHM1 (S432/S435)
total PLEKHM1
pERK1/2 (T202/Y204)
total ERK1/2
pS6K (T389)
total S6K
E
MEFs + HA-PLEKHM1
V
FM
Torin1
U0126
Starve
130 kDa
130 kDa
35 kDa
35 kDa
75 kDa
75 kDa
pPLEK (S432/S435)
Total PLEKHM1
pERK1/2 (T202/Y204)
Total ERK1/2
p-p70S6K (T389)
Total p70S6K
F
% Phsopho PLEKHM1 (pSer/Total)
150
100
50
0
**
***
*
*
****
****
FM
Torin1
UO126
Torin 1+ UO126
EBSS

pathway, as reflected in the levels of phosphorylated ERK (phospho-ERK1/2) after a 30-minute stimulation (Fig. 4B). As the sites conformed to the MAPK consensus sequence and phosphorylation of PLEKHM1 followed that of ERK1/2 activation (Fig. 4B), we next tested whether PLEKHM1 could be directly phosphorylated by MAPK1 (ERK2). Using GST-PLEKHM1 (418-456, Fig. 3F), we incubated recombinant MKK1 (MEK) alone, MAPK1 WT alone, MKK plus MAPK1 and MKK1 plus kinase dead MAPK1 (D168A), in the presence or absence of ATP. Under these conditions, PLEKHM1 is directly phosphorylated by MAPK1 at Ser432/Ser435 only in the presence of ATP (Fig. 4C, lanes 3 and 5), but not by MKK1 alone (Fig. 4C, lane 1) or by kinase dead MAPK (Fig. 4C, lanes 6 and 7). Next, we wanted to test the specificity of such response by applying a number of different growth factor conditions in combination with the inhibition of MAPK and mTOR pathways and subsequently probing the levels of phosphorylated PLEKHM1 at the phosphospecific sites. MEFs expressing HA-tagged PLEKHM1 were grown overnight in 1% serum and stimulated in the presence or absence of 10 μM U0126 or 250 nM torin 1 with either EGF (epidermal growth factor), FGF2 (fibroblast growth factor 2), IGF-1 (Insulin-like growth factor 1), PDGF-AA (Platelet-derived growth factor-AA), PDGF-BB or PDGF-AB for 30 min. Using phospho-ERK1/2 (Thr202/Tyr204) and phospho-p70S6K (T389), as a read-out MAPK and mTOR activity, respectively, we observed a robust phosphorylation (>2-fold increase in phospho-PLEKHM1 compared with unstimulated) of PLEKHM1 at Ser432/435 treated with EGF, FGF2 and PDGF-AB (Fig. 4D). FGF2-mediated PLEKHM1 phosphorylation was partially (approx. 40%) sensitive to MAPK inhibition, but not to mTOR inhibition (Figs 4D and S3). Next, we wanted to assess the relative contributions of the mTOR and MAPK pathways to Ser432/Ser435 phosphorylation. Stimulation of MEFs containing HA-PLEKHM1 with full medium resulted in a robust phosphorylation at Ser432/Ser435, while treatment with the mTOR inhibitor torin 1 resulted in an approximate 50% decrease (Fig. 4E, F). Treatment with U0126 resulted in a 60% decrease, and inhibition of both MAPK and mTOR resulted in an almost complete loss of PLEKHM1 phosphorylation, similar to that observed after a 4-h starvation (EBSS medium; Fig. 4E, F). This indicates that both the mTOR and the MAPK pathways can phosphorylate directly PLEKHM1 at Ser432/Ser435, pointing to a convergence of pathways for a function that has yet to be determined.

Discussion

The late endocytic adaptor protein PLEKHM1, which is involved in osteoclast vesicle transport [41] through an interaction with Rab7 [24–26], plays an important role in the maturation of late endosomes [24,26,27], biogenesis of the *Salmonella*-containing vacuole [25] and fusion of autophagosomes and lysosomes [26,37,42]. How these distinct, yet related, functions are regulated was unclear. Herein, we discover post-translational modification of human PLEKHM1 in a highly conserved region spanning amino acids 420–450. Phosphorylation of serine residues in a proline-directed manner is carried out directly by mTOR kinase, a binding partner of PLEKHM1. Interestingly, it has recently been shown that mTORC2 complex in *C. elegans* influences autophagosome biogenesis [43]. Since we also found mTORC2 components coprecipitating with PLEKHM1 (Fig. 1A,B), we cannot rule out a role for mTORC2-mediated PLEKHM1 phosphorylation at S432/S435. We additionally show that the very same sites that are targeted by mTOR are also targets for the MAPK pathway; hence, the inhibition of both MAPK and mTOR results in a complete loss of phosphorylated PLEKHM1 at these sites. This indicates that PLEKHM1 functions at the crossroads of these two signalling pathways and potentially integrates them into unique cellular response reflected in specific dynamics of autophagosome-lysosome fusion (mTOR pathway) or growth factor receptor degradation (MAPK pathway), depending on cell type and function, as well as on physiological demands.

Regulation of adaptor and receptor proteins in both autophagy and the endocytic pathway is an emerging topic in how cells fine-tune their responses to stress, and current data are highly supportive of phosphorylation as an important regulatory mechanism. For example, during selective autophagy, the receptor proteins optineurin and p62/SQSTM1 can both target ubiquitinated *Salmonella* for destruction by the autophagosome-to-lysosome pathway [44,45]. Interestingly, both are phosphorylated by TBK1 to either enhance MAP1LC3B interaction [45,46], enhance the interaction with ubiquitinated *Salmonella* [47,48] or increased activation of oxidative stress pathways [49]. This modifiable switch helps in the mobilization and activation of receptor activity, rendering it more effective in the clearance of intracellular pathogens. In addition to autophagy receptors, adaptor proteins that control formation, trafficking and fusion of autophagosomes can also be regulated in a similar manner. One such example is protein Rubicon, which shares a high degree of homology with PLEKHM1, is phosphorylated by

HUNK at two serine residues in the region that binds Vps34 and regulates the autophagy-suppressive function of Rubicon [50].

PLEKHM1 is phosphorylated at Ser432/Ser435 under normal growth conditions, but becomes rapidly dephosphorylated under starvation conditions or upon chemically induced inhibition of mTOR. As part of our studies, we used doxycycline-inducible system for the induction of overexpressed PLEKHM1. Although we saw very little change in mTOR activity after doxycycline addition, any potential metabolic changes caused by the doxycycline may need to be explored in future studies [51]. Potentially, there could be rapidly acting phosphatases that change the dynamic pool of phosphorylated PLEKHM1 that could affect the dynamics of PLEKHM1-mediated fusion events in the cells depending on the cellular demand. This pointed towards high sensitivity of PLEKHM1 to the activity of mTOR and physiological state of the cell.

In this study, our proteomics data correlates with previous reports of multiple deep-sequence mass spectrometry analyses (www.phosphosite.org). The phosphosites are located within a highly conserved unstructured region of PLEKHM1 and our data suggests an involvement of major metabolic kinases in regulation of PLEKMH1 (Fig. 2H). In order to study this regulation in more detail, we have developed several tools to study these mechanisms, including a phospho-specific antibody that detects a double-serine phosphorylation motif on PLEKHM1 (S432/S435). In combination with CRISPR/Cas9-mediated endogenous tagging of PLEKHM1 (Figure S1 and 1C), these tools will enable us to challenge the cells with broader set of chemical compounds and directly test both post-translational modifications, as well as interacting partners of PLEKHM1 in a systematic top-down approach. Further, combining such approaches will allow us, and others, to accurately detect and quantify levels and spatial organization of phosphorylated PLEKHM1 in various cell types and stress conditions. This will help expand our understanding of the interconnectivity between autophagy and growth factor receptor signalling.

Similar to the examples of other autophagy adaptors, our data suggest that the function of phosphosites in PLEKHM1 could be regulation of interactions of PLEKHM1 with components of the lysosome. Under conditions of starvation or inhibition of mTOR, mTOR dissociates from LAMP2-positive structures, but PLEKHM1 remains associated (Fig. 1E). Interestingly, mutation of PLEKHM1 at Ser432/435 did not affect the known interaction with GABARAP (Fig. S2A,B) [24,25,41] or Rab7 (Fig. S2C-D) [24,25,41] and so potentially does not function in these distal interactions. However, we cannot rule out any changes in the interaction with HOPS/SNARE complex [26] or the recently identified interaction with Arl8b that was mapped to the RUN domain [27], which is in close proximity to phosphoserine Ser432/Ser435 site. These phosphosites may, therefore, act as on/off switch for PLEKHM1 function during conditions such as cellular stress. In addition, we also showed that these sites are not only a direct target for mTOR, but that they also share similarities with a MAPK PxSP motif and are sensitive to MAPK inhibition alone. Indeed, phosphorylation of PLEKHM1 at Ser432/Ser435 was induced by certain growth factors via both MAPK-dependent (EGF, FGF2, IGF-1) and MAPK-independent (PDGF-BB, PDGF-AB) manner, indicating compartmentalization of PLEKHM1 function. These data firmly position PLEKHM1 regulation at the crossroads of two major growth and proliferative signal transduction pathways and, given our previous findings showing that PLEKHM1 is required for both autophagosome and EGFR degradation [26], our results shed some light on possible mechanisms that may govern its activity. These early findings will help pave a way to dissect how these signalling pathways converge and regulate the function of this adaptor protein at the molecular level.

Acknowledgements

The anti-LAMP-2 (H4B4) antibody was obtained from the Developmental Studies Hybridoma Bank, created by the NICHD of the NIH and maintained at The University of Iowa. This work was supported by grants from Tenovus Scotland (T16/44) and a Wellcome Trust Seed Award (202061/Z/16/Z) to DGM and institutional funds of the Georg-Speyer-Haus to D.S.K. The Georg-Speyer-Haus is funded jointly by the German Federal Ministry of Health (BMG) and the Ministry of Higher Education, Research and the Arts of the State of Hessen (HMWK).

Author contributions

CK, DP and AP performed and analysed experiments. GT and MEH analysed mass spectrometry data, and ND provided technical support. ID and DSK provided feedback and support during the experimental and writing procedures. AG and DGM designed, performed and analysed experiments and wrote the manuscript.

References

1 Saxton RA and Sabatini DM (2017) mTOR signaling in growth, metabolism, and disease. *Cell* **169**, 361–371.

2 Lemmon MA and Schlessinger J (2010) Cell signaling by receptor tyrosine kinases. *Cell* **141**, 1117–1134.

3 Braicu C, Buse M, Busuioc C, Drula R, Gulei D, Raduly L, Rusu A, Irimie A, Atanasov AG, Slaby O *et al.* (2019) A comprehensive review on MAPK: a promising therapeutic target in cancer. *Cancers (Basel)* **11,** 1618.

4 Kim DH, Sarbassov DD, Ali SM, Latek RR, Guntur KVP, Erdjument-Bromage H, Tempst P and Sabatini DM (2003) GβL, a positive regulator of the rapamycin-sensitive pathway required for the nutrient-sensitive interaction between raptor and mTOR. *Mol Cell* **11**, 895–904.

5 Peterson TR, Laplante M, Thoreen CC, Sancak Y, Kang SA, Kuehl WM, Gray NS and Sabatini DM (2009) DEPTOR is an mTOR inhibitor frequently overexpressed in multiple myeloma cells and required for their survival. *Cell* **137**, 873–886.

6 Kim DH, Sarbassov DD, Ali SM, King JE, Latek RR, Erdjument-Bromage H, Tempst P and Sabatini DM (2002) mTOR interacts with raptor to form a nutrient-sensitive complex that signals to the cell growth machinery. *Cell* **110**, 163–175.

7 Hara K, Maruki Y, Long X, Yoshino K, Oshiro N, Hidayat S, Tokunaga C, Avruch J and Yonezawa K (2002) Raptor, a binding partner of target of rapamycin (TOR), mediates TOR action. *Cell* **110**, 177–189.

8 Kim DH and Sabatini DM (2003) Raptor and mTOR: Subunits of a nutrient-sensitive complex. *Curr Top Microbiol Immunol* **279**, 259–270.

9 Sancak Y, Thoreen CC, Peterson TR, Lindquist RA, Kang SA, Spooner E, Carr SA and Sabatini DM (2007) PRAS40 is an insulin-regulated inhibitor of the mTORC1 protein kinase. *Mol Cell* **25**, 903–915.

10 Sarbassov DD, Ali SM, Kim D-H, Guertin DA, Latek RR, Erdjument-Bromage H, Tempst P and Sabatini DM (2004) Rictor, a novel binding partner of mTOR, defines a rapamycin-insensitive and raptor-independent pathway that regulates the cytoskeleton dos. *Curr Biol* **4**, 1296–1302.

11 Frias MA, Thoreen CC, Jaffe JD, Schroder W, Sculley T, Carr SA and Sabatini DM (2006) mSin1 is necessary for Akt/PKB phosphorylation, and its isoforms define three distinct mTORC2s. *Curr Biol* **16**, 1865–1870.

12 Pearce LR, Huang X, Boudeau J, Pawłowski R, Wullschleger S, Deak M, Ibrahim AFM, Gourlay R, Magnuson MA and Alessi DR (2007) Identification of protor as a novel Rictor-binding component of mTOR complex-2. *Biochem J* **405**, 513–522.

13 Sancak Y, Bar-Peled L, Zoncu R, Markhard AL, Nada S and Sabatini DM (2010) Ragulator-rag complex targets mTORC1 to the lysosomal surface and is necessary for its activation by amino acids. *Cell* **141**, 290–303.

14 Sarbassov DD, Guertin DA, Ali SM and Sabatini DM (2005) Phosphorylation and regulation of Akt/PKB by the rictor-mTOR complex. *Science (80-* **) 307**, 1098–1101.

15 Tato I, Bartrons R, Ventura F and Rosa JL (2011) Amino acids activate mammalian target of rapamycin complex 2 (mTORC2) via PI3K/Akt signaling. *J Biol Chem* **286**, 6128–6142.

16 Hosokawa N, Hara T, Kaizuka T, Kishi C, Takamura A, Miura Y, Iemura SI, Natsume T, Takehana K, Yamada N *et al.* (2009) Nutrient-dependent mTORCl association with the ULK1-Atg13-FIP200 complex required for autophagy. *Mol Biol Cell* **20**, 1981–1991.

17 Kim J, Kundu M, Viollet B and Guan KL (2011) AMPK and mTOR regulate autophagy through direct phosphorylation of Ulk1. *Nat Cell Biol* **13**, 132–141.

18 Bach M, Larance M, James DE and Ramm G (2011) The serine/threonine kinase ULK1 is a target of multiple phosphorylation events. *Biochem J* **440**, 283–291.

19 Liu CC, Lin YC, Chen YH, Chen CM, Pang LY, Chen HA, Wu PR, Lin MY, Jiang ST, Tsai TF and *et al.* (2016) Cul3-KLHL20 ubiquitin ligase governs the turnover of ULK1 and VPS34 complexes to control autophagy termination. *Mol Cell* **61**, 84–97.

20 Li TY, Sun Y, Liang Y, Liu Q, Shi Y, Zhang CS, Zhang C, Song L, Zhang P, Zhang X *et al.* (2016) ULK1/2 constitute a bifurcate node controlling glucose metabolic fluxes in addition to autophagy. *Mol Cell* **62**, 359–370.

21 Egan DF, Chun MGH, Vamos M, Zou H, Rong J, Miller CJ, Lou HJ, Raveendra-Panickar D, Yang CC, Sheffler DJ *et al.* (2015) Small molecule inhibition of the autophagy kinase ULK1 and identification of ULK1 substrates. *Mol Cell* **59**, 285–297.

22 Russell RC, Tian Y, Yuan H, Park HW, Chang YY, Kim J, Kim H, Neufeld TP, Dillin A and Guan KL (2013) ULK1 induces autophagy by phosphorylating Beclin-1 and activating VPS34 lipid kinase. *Nat Cell Biol* **15**, 741–750.

23 Mercer TJ, Gubas A and Tooze SA (2018) A molecular perspective of mammalian autophagosome biogenesis. *J Biol Chem* **293,** 5386–5395.

24 Tabata K, Matsunaga K, Sakane A, Sasaki T, Noda T and Yoshimori T (2010) Rubicon and PLEKHM1 negatively regulate the endocytic/autophagic pathway via a novel Rab7-binding domain. *Mol Biol Cell* **21**, 4162–4172.

25 McEwan DG, Richter B, Claudi B, Wigge C, Wild P, Farhan H, McGourty K, Coxon FP, Franz-Wachtel M, Perdu B *et al.* (2015) PLEKHM1 regulates salmonella-containing vacuole biogenesis and infection. *Cell Host Microbe* **17**, 58–71.

26 McEwan DG, Popovic D, Gubas A, Terawaki S, Suzuki H, Stadel D, Coxon FP, MirandadeStegmann D, Bhogaraju S, Maddi K *et al.* (2015) PLEKHM1 regulates autophagosome-lysosome fusion through HOPS complex and LC3/GABARAP proteins. *Mol Cell* **57**, 39–54.
27 Marwaha R, Arya SB, Jagga D, Kaur H, Tuli A and Sharma M (2017) The Rab7 effector PLE KHM1 binds Arl8b to promote cargo traffic to lysosomes. *J Cell Biol* **216**, 1051–1070.
28 Thoreen CC, Kang SA, Chang JW, Liu Q, Zhang J, Gao Y, Reichling LJ, Sim T, Sabatini DM and Gray NS (2009) An ATP-competitive mammalian target of rapamycin inhibitor reveals rapamycin-resistant functions of mTORC1. *J Biol Chem* **284**, 8023–8032.
29 García-Martínez JM, Moran J, Clarke RG, Gray A, Cosulich SC, Chresta CM and Alessi DR (2009) Ku-0063794 is a specific inhibitor of the mammalian target of rapamycin (mTOR). *Biochem J* **421**, 29–42.
30 Kinoshita E, Kinoshita-Kikuta E, Takiyama K and Koike T (2006) Phosphate-binding tag, a new tool to visualize phosphorylated proteins. *Mol Cell Proteomics* **5**, 749–757.
31 Sharma K, D'Souza RCJ, Tyanova S, Schaab C, Wiśniewski JR, Cox J and Mann M (2014) Ultradeep human Phosphoproteome Reveals a Distinct Regulatory Nature of Tyr and Ser/Thr-Based Signaling. *Cell Rep* **8**, 1583–1594.
32 Yi T, Zhai B, Yu Y, Kiyotsugu Y, Raschle T, Etzkorn M, Seo HC, Nagiec M, Luna RE, Reinherz EL *et al.* (2014) Quantitative phosphoproteomic analysis reveals system-wide signaling pathways downstream of SDF-1/CXCR4 in breast cancer stem cells. *Proc Natl Acad Sci U S A* **111**, E2182–E2190.
33 Schweppe DK, Rigas JR and Gerber SA (2013) Quantitative phosphoproteomic profiling of human non-small cell lung cancer tumors. *J Proteomics* **91**, 286–296.
34 Weber C, Schreiber TB and Daub H (2012) Dual phosphoproteomics and chemical proteomics analysis of erlotinib and gefitinib interference in acute myeloid leukemia cells. *J Proteomics* **75**, 1343–1356.
35 Yu Y, Yoon SO, Poulogiannis G, Yang Q, Ma XM, Villén J, Kubica N, Hoffman GR, Cantley LC, Gygi SP *et al.* (2011) Phosphoproteomic analysis identifies Grb10 as an mTORC1 substrate that negatively regulates insulin signaling. *Science (80-)* **332**, 1322–1326.
36 Humphrey SJ, Yang G, Yang P, Fazakerley DJ, Stöckli J, Yang JY and James DE (2013) Dynamic adipocyte phosphoproteome reveals that akt directly regulates mTORC2. *Cell Metab* **17**, 1009–1020.
37 Rogov VV, Stolz A, Ravichandran AC, Rios-Szwed DO, Suzuki H, Kniss A, Löhr F, Wakatsuki S, Dötsch V, Dikic I *et al.* (2017) Structural and functional analysis of the GABARAP interaction motif (GIM). *EMBO Rep* **18**, 1382–1396.
38 Hsu PP, Kang SA, Rameseder J, Zhang Y, Ottina KA, Lim D, Peterson TR, Choi Y, Gray NS, Yaffe MB *et al.* (2011) The mTOR-regulated phosphoproteome reveals a mechanism of mTORC1-mediated inhibition of growth factor signaling. *Science (80-)* **332**, 1317–1322.
39 Songyang Z, Lu KP, Kwon YT, Tsai LH, Filhol O, Cochet C, Brickey DA, Soderling TR, Bartleson C, Graves DJ *et al.* (1996) A structural basis for substrate specificities of protein Ser/Thr kinases: primary sequence preference of casein kinases I and II, NIMA, phosphorylase kinase, calmodulin-dependent kinase II, CDK5, and Erk1. *Mol Cell Biol* **16**, 6486–6493.
40 Pearson G, Robinson F, Beers Gibson T, Xu B, Karandikar M, Berman K and Cobb MH (2001) Mitogen-Activated Protein (MAP) kinase pathways: regulation and physiological functions*. *Endocr Rev* **22**, 153–183.
41 Van Wesenbeeck L, Odgren PR, Coxon FP, Frattini A, Moens P, Perdu B, MacKay CA,Van Hul E, Timmermans JP, Vanhoenacker F, Jacobs R, Peruzzi B, Teti A, Helfrich MH, Rogers MJ, Villa A & Van Hul W (2007) Involvement of PLEKHM1 in osteoclastic vesicular transport and osteopetrosis in incisors absent rats and humans. *J Clin Invest* 117, 919–930.
42 Nguyen TN, Padman BS, Usher J, Oorschot V, Ramm G and Lazarou M (2016) Atg8 family LC3/GAB ARAP proteins are crucial for autophagosome-lysosome fusion but not autophagosome formation during PINK1/Parkin mitophagy and starvation. *J Cell Biol* **215**, 857–874.
43 Aspernig H, Heimbucher T, Qi W, Gangurde D, Curic S, Yan Y, Donner von Gromoff E, Baumeister R and Thien A (2019) Mitochondrial perturbations couple mTORC2 to autophagy in C. elegans. *Cell Rep* **29**, 1399–1409.e5.
44 Mostowy S, Sancho-Shimizu V, Hamon MA, Simeone R, Brosch R, Johansen T and Cossart P (2011) p62 and NDP52 proteins target intracytosolic Shigella and Listeria to different autophagy pathways. *J Biol Chem* **286**, 26987–26995.
45 Wild P, Farhan H, McEwan DG, Wagner S, Rogov VV, Brady NR, Richter B, Korac J, Waidmann O, Choudhary C *et al.* (2011) Phosphorylation of the autophagy receptor optineurin restricts Salmonella growth. *Science (80-)* **333**, 228–233.
46 Rogov VV, Suzuki H, Fiskin E, Wild P, Kniss A, Rozenknop A, Kato R, Kawasaki M, McEwan DG, Löhr F *et al.* (2013) Structural basis for phosphorylation-triggered autophagic clearance of Salmonella. *Biochem J* **454**, 459–466.
47 Matsumoto G, Wada K, Okuno M, Kurosawa M and Nukina N (2011) Serine 403 phosphorylation of p62/

SQSTM1 regulates selective autophagic clearance of ubiquitinated proteins. *Mol Cell* **44**, 279–289.
48 Pilli M, Arko-Mensah J, Ponpuak M, Roberts E, Master S, Mandell MA, Dupont N, Ornatowski W, Jiang S, Bradfute SB *et al.* (2012) TBK-1 promotes autophagy-mediated antimicrobial defense by controlling autophagosome maturation. *Immunity* **37**, 223–234.
49 Ishimura R, Tanaka K and Komatsu M (2014) Dissection of the role of p62/Sqstm1 in activation of Nrf2 during xenophagy. *FEBS Lett* **588**, 822–828.
50 Zambrano JN, Eblen ST, Abt M, Rhett JM, Muise-Helmericks R and Yeh ES (2019) HUNK phosphorylates rubicon to support autophagy. *Int J Mol Sci* **20**. https://www.mdpi.com/1422-0067/20/22/5813/htm
51 Chatzispyrou IA, Held NM, Mouchiroud L, Auwerx J and Houtkooper RH (2015) Tetracycline antibiotics impair mitochondrial function and its experimental use confounds research. *Cancer Res* **75**, 4446–4449.
52 Neumann B, Held M, Liebel U, Erfle H, Rogers P, Pepperkok R and Ellenberg J (2006) High-throughput RNAi screening by time-lapse imaging of live human cells. *Nat Methods* **3**, 385–390.
53 Cox J, Neuhauser N, Michalski A, Scheltema RA, Olsen JV and Mann M (2011) Andromeda: a peptide search engine integrated into the MaxQuant environment. *J Proteome Res* **10**, 1794–1805.
54 Tyanova S, Temu T and Cox J (2016) The MaxQuant computational platform for mass spectrometry-based shotgun proteomics. *Nat Protoc* **11**, 2301–2319.
55 Elias JE and Gygi SP (2007) Target-decoy search strategy for increased confidence in large-scale protein identifications by mass spectrometry. *Nat Methods* **4**, 207–214.
56 Schindelin J, Arganda-Carreras I, Frise E, Kaynig V, Longair M, Pietzsch T, Preibisch S, Rueden C, Saalfeld S, Schmid B *et al.* (2012) Fiji: An open-source platform for biological-image analysis. *Nat Methods* **9**, 676–682.

Supporting information

Additional supporting information may be found online in the Supporting Information section at the end of the article.

Fig. S1. (A) U2OS cells modified using CRISPR/Cas9 plasmids showing parental (WT) PLEKHM1 KO and GFP-tagged endogenous PLEKHM1. Total cell lysates were probed with anti-PLEKHm1 and vinculin for loading. (B) Mass spectra for PLEKHM1 phosphopeptides that changed upon either starvation or 10 μM Ku-0063794 and shown are shown for Ser432, Thr434 (C), Ser435 (D), Ser224 (E), Ser305 (F) and Ser501 (G).

Fig. S2. (A) HEK293T cells overexpressing HA-tagged PLEKHM1 WT, PLEKHM1 S432A/S435A (2A) or PLEKHM1 S432D/S435D (2D) were co-expressed with either GFP alone or GFP-Rab7. Anti-GFP beads were used to precipitate the GFP-tag and samples were probed with ant-HA and anti-GFP antibodies. (B) Quantification of (A) over n=3 independent experiments shows no significant difference in the interaction of PLEKHM1 with GFP-Rab7 using students t-test. Mean ± S.D shown. (C) HEK293T cells overexpressing HA-tagged PLEKHM1 WT, -PLEKHM1-2A or PLEKHM1-2D were co-expressed with either GFP alone or GFP-GABARAP. Anti-GFP beads were used to precipitate the GFP-tag and samples were probed with ant-HA and anti-GFP antibodies. (D) Quantification of (C) over n=3 independent experiments shows no significant difference in the interaction of PLEKHM1 with GFP-Rab7 using students t-test. Mean ± SD shown. (E) HEK293T cells transiently overexpressing either empty vector HA-tagged PLEKHM1 WT, PLEKHM1 S432A/S435A (2A) or PLEKHM1 S432D/S435D (2D) were kept in either full media (F) or treated with 200nM BafilomycinA1 (B) or starved (S; EBSS media) for 2 hours. Cells were lysed in total cell lysis buffer and subjected to SDS-PAGE and western blot analysis. Membranes were probed with anti-HA (PLEKHM1), anti-LC3B, anti-p62/SQSTM1 and anti-vinculin as loading control. F. Results from (E) were then quantified and fold change of LC3B-II and p62 (G) were normalized to vinculin loading. Shown is the mead ± S.D. of $n = 3$ independent experiments (represented by individual points) on the scatter plots. Significance was calculated using one-way ANOVA, but no significant differences were observed between conditions.

Fig. S3. Quantification of phosphorylation of PLEKHM1 under growth factor stimulation ± torin1 or ±U0126 (related to Figure 4D). Fold change of phospho-PLEKHM1 (S432/S435) normalized to total PLEKHM1. Data represents mean ± SEM of $n = 3$ independent biological repeats. Statistical significance calculated using One-way ANOVA. * $p = 0.0299$ (NT vs FGF2); $p = 0.1083$ (ns; NT vs FGF2+U0126); $p = 0.0428$; $p = 0.0105$ (FGF2 vs FGF2+U0126) ; $p = 0.0146$ (FGF2 vs FGF2 + torin1); $p = 0.0163$ (FGF2 + U0126 vs FGF2 + torin1).

Table S1. Plasmids used in this study.